

# 000 001 002 003 004 005 006 007 008 009 010 011 012 013 014 015 016 017 018 019 020 021 022 023 024 025 026 027 028 029 030 031 032 033 034 035 036 037 038 039 040 041 042 043 044 045 046 047 048 049 050 051 052 053 ERROR PROPAGATION IN DYNAMIC PROGRAMMING: FROM STOCHASTIC CONTROL TO OPTION PRICING

Anonymous authors

Paper under double-blind review

## ABSTRACT

This paper investigates theoretical and methodological foundations for stochastic optimal control (SOC) in discrete time. We start formulating the control problem in a general dynamic programming framework, introducing the mathematical structure needed for a detailed convergence analysis. The associate value function is estimated through a sequence of approximations combining nonparametric regression methods and Monte Carlo subsampling. The regression step is performed within reproducing kernel Hilbert spaces (RKHSs), exploiting the classical KRR algorithm, while Monte Carlo sampling methods are introduced to estimate the continuation value. To assess the accuracy of our value function estimator, we propose a natural error decomposition and rigorously control the resulting error terms at each time step. We then analyze how this error propagates backward in time—from maturity to the initial stage—a relatively underexplored aspect of the SOC literature. Finally, we illustrate how our analysis naturally applies to a key financial application: the pricing of American options.

## 1 INTRODUCTION AND RELATED WORK

Stochastic optimal control (SOC) provides a principled framework for sequential decision-making under uncertainty. It plays a foundational role in a wide range of scientific and engineering domains, including economics and finance (Fleming & Stein, 2004; Pham, 2009; Åström, 2012), robotics (Gorodetsky et al., 2018; Theodorou et al., 2011), molecular dynamics (Hartmann & Schütte, 2012; Hartmann et al., 2013; Zhang et al., 2014; Holdijk et al., 2023), and stochastic filtering and data assimilation (Mitter, 2002; Reich, 2019). More recently, SOC has inspired advances in machine learning, particularly in tasks such as sampling from unnormalized distributions (Zhang & Chen, 2021; Berner et al., 2022; Richter & Berner, 2023; Vargas et al., 2023), nonconvex optimization (Chaudhari et al., 2018), optimal transport (Villani et al., 2008), and the numerical solution of backward stochastic differential equations (BSDEs) (Carmona, 2016).

Despite the extensive literature on continuous-time SOC (Bertsekas, 2012), its discrete-time counterpart remains highly relevant in practice, as it naturally arises in computational and data-driven settings where decisions are made at fixed time intervals (Bertsekas & Shreve, 1996; Hernández-Lerma & Lasserre, 2012; Puterman, 2014). At the same time, discrete-time SOC poses distinct challenges, largely because many of the analytical tools available in continuous time are no longer applicable. Nevertheless, it still offers opportunities for the development of scalable numerical methods, particularly through dynamic programming and function approximation. Discrete-time SOC is central to modern applications in operations research, financial engineering or reinforcement learning (RL) (Sutton et al., 1998). At its core lies a dynamic programming (DP) recursion, where the value function is computed backward in time via the Bellman operator (Bellman, 1966). In high-dimensional settings, solving this recursion exactly is often infeasible, inspiring a large body of research focused on developing scalable and efficient approximations. These approaches typically estimate value functions from data using simulation or function approximation. In recent years, deep learning has greatly expanded the scalability of these methods, enabling their application to high-dimensional control problems (Han et al., 2016; Domingo i Enrich et al., 2024).

Despite this empirical progress, the theoretical understanding of learning-based SOC remains limited. A key challenge lies in quantifying how local errors deriving from function approximation, sampling noise, or optimization inaccuracies, propagate through the Bellman recursion over time.

054 Studying this requires a rigorous and principled mathematical framework in which to analyze error  
 055 accumulation in high-dimensional value function approximations. In this work, we propose such a  
 056 framework based on reproducing kernel Hilbert spaces (RKHS), which enables us to derive explicit  
 057 error bounds and control error propagation in approximate dynamic programming.

058 A classical application of discrete-time SOC is the pricing of American-style options, also known  
 059 as Bermudan options when exercise opportunities are discrete. This problem can be formulated  
 060 as a finite-horizon optimal stopping problem under stochastic dynamics. While such problems  
 061 can, in principle, be solved exactly (Peskir & Shiryaev, 2006; Lamberton & Lapeyre, 2011), well-  
 062 established numerical methods, such as tree-based approaches or PDE solvers, struggle with the  
 063 curse of dimensionality as complexity increases (Broadie & Glasserman, 1997; Bally et al., 2003;  
 064 Jain & Oosterlee, 2012). Monte Carlo-based methods have become widespread in high-dimensional  
 065 applications. Notable examples include regression-based techniques (Tsitsiklis & Van Roy, 1999;  
 066 Longstaff & Schwartz, 2001), dual and hybrid primal-dual formulations (Rogers, 2002; Haugh &  
 067 Kogan, 2004; Andersen & Broadie, 2004; Belomestny et al., 2013; Lelong, 2018), and Malliavin calculus  
 068 methods for estimating conditional expectations (Lions & Regnier, 2001; Bouchard & Touzi,  
 069 2004; Bally et al., 2005; Abbas-Turki & Lapeyre, 2012). More recently, machine learning (Williams  
 070 & Rasmussen, 2006) and deep learning approaches (Kohler et al., 2010; Nielsen, 2015; Becker et al.,  
 071 2019; Goudenege et al., 2020) have shown strong empirical performance in this domain. However,  
 072 these methods often lack rigorous theoretical guarantees on accuracy and generalization.

073 Our work aims to bridge this gap by developing kernel-based algorithms for discrete-time SOC that  
 074 come with provable convergence guarantees and theoretical error bounds, while keeping an eye on  
 075 computational efficiency and scalability for big data applications.

076 **Contribution** In summary, our contributions are as follows. First, we propose a general RKHS-  
 077 based formulation of approximate dynamic programming through backward induction. Second, we  
 078 provide a rigorous and transparent decomposition of the total approximation error into three distinct  
 079 components: regression error, Monte-Carlo sampling error, and propagation error. Third, we derive  
 080 explicit convergence rates under model misspecification by leveraging source conditions. Finally, we  
 081 show how this framework can be applied to various problems, especially in finance. We demonstrate  
 082 the practical effectiveness of our algorithm through the well-known problem of American option  
 083 pricing and preliminarily test its performance against some of the standard benchmark methods in  
 084 the field.

085 **Organization** The paper is organized as follows. In Section 2 we introduce the problem and  
 086 setting, with key definitions and notations used throughout the paper, and formalizing the problem  
 087 in a precise mathematical framework. In Section 3 we introduce the Monte Carlo approximation  
 088 and the regression step in the RHKS environment. In Section 4 we study the error back-propagation,  
 089 upper bounding the various approximation terms and finally showing the final error guarantees in  
 090 Theorem 1. In Section 5 we finally present some numerical results.

## 092 2 SETTING AND STOCHASTIC CONTROL MODEL

093 Consider a discrete time horizon  $t = \{0, 1, \dots, T\}$ . We define a stochastic process  $Z := (Z_t)_{t=0}^T$  on  
 094 a filtered probability space  $(\Omega, \mathcal{F}, (\mathcal{F}_t^Z)_{t=0}^T, \mathbb{P})$ , where  $(\mathcal{F}_t^Z)_{t=0}^T$  is the natural filtration generated by  
 095  $Z$ . The random variables  $Z_t$  are mutually independent (but not necessarily identically distributed)  
 096 and take values in measurable spaces  $\mathcal{Z}_t$ . We denote by  $\mathbb{P}(dz) = \prod_{t=0}^T \mathbb{P}_t(dz_t)$  the distribution  
 097 of  $Z$  on the path space  $\mathcal{Z} = \mathcal{Z}_0 \times \dots \times \mathcal{Z}_T$ , which we identify with  $\Omega$  without loss of generality.  
 098 Any square-integrable adapted process, such as an asset price process, can be written in the form  
 099  $X_t = X_t(Z_0, \dots, Z_t)$ , for some function  $X_t \in L^2_{\mathbb{P}_0 \times \dots \times \mathbb{P}_t}$ .

100 Controlled Markov process  $X_0^u, \dots, X_T^u$  taking values in state spaces  $\mathcal{X}_0, \dots, \mathcal{X}_T$  is defined by  
 101

$$\begin{cases} X_0^u = p_0(Z_0), \\ X_{t+1}^u = \pi_t(X_t^u, u_t(X_t^u), Z_{t+1}), \end{cases} \quad t \in \{0, \dots, T-1\}, \quad (1)$$

102 where  $p_0 : \mathcal{Z}_0 \rightarrow \mathcal{X}_0$  is the initial state distribution,  $\pi_t : \mathcal{X}_t \times \mathcal{U}_t \times \mathcal{Z}_{t+1} \rightarrow \mathcal{X}_{t+1}$  is a Markov transition  
 103 function encoding how the system transitions from one state to the next, and  $\mathbf{u} = (u_t)_{t=0}^{T-1} \in \mathcal{U}$   
 104 is a stochastic control law, where each  $u_t : \mathcal{X}_t \rightarrow \mathcal{U}_t$  is  $\mathcal{F}_t$ -measurable.

108 **Remark 1.** Note that this setup remains very general despite the Markovian assumption. For rea-  
 109 sons related to dimensionality, it is typically assumed that  $X_t^u$  summarizes the full history  $Z_{0:t}, u_{0:t}$   
 110 in a compressed form, so that the control at time  $t$  depends only on  $X_t^u$ , i.e.,  $u_t = u_t(X_t^u)$ . This does  
 111 not entail a loss of generality, as many important problems are naturally Markovian. Moreover, any  
 112 optimal stopping problem can be cast in Markovian form by including all relevant past information  
 113 in the current state, at the cost of increasing dimensionality.

114 A control law  $u$  is said to be *admissible* if the maps  $(x, z) \mapsto \pi_t(x, u_t(x), z)$  satisfy suitable regu-  
 115 larity conditions. In particular, we assume that the operator  
 116

$$117 \quad P_t^u f(x) := \mathbb{E} [f(X_{t+1}^u) \mid X_t^u = x] = \mathbb{E} [f(\pi_t(x, u, Z_{t+1}))] = \int_{\mathcal{Z}_{t+1}} f(\pi_t(x, u, z)) \mathbb{P}_{t+1}(dz), \\ 118 \quad (2)$$

120 defines a Markov transition kernel from  $\mathcal{X}_t$  to  $\mathcal{X}_{t+1}$ , for all  $u \in \mathcal{U}_t$ . With a slight abuse of notation,  
 121 we will sometimes use the alternative, also common definition in kernel form

$$122 \quad P_t^u(x, A) := \mathbb{P} [X_{t+1}^u \in A \mid X_t^u = x] = \int_{\mathcal{Z}_{t+1}} \mathbb{1}_A(\pi_t(x, u, z)) \mathbb{P}_{t+1}(dz) \\ 123 \quad (3)$$

125 with  $A \in \mathcal{B}(\mathcal{X}_{t+1})$ , i.e. the Borel  $\sigma$ -algebra on the space  $\mathcal{X}_{t+1}$ . In the following, it will be clear  
 126 which one of the two representations we are using. The connection between the two is simply

$$127 \quad P_t^u f(x) = \int_{\mathcal{X}_{t+1}} f(x') P_t^u(x, dx'). \\ 128 \quad (4)$$

130 The objective of stochastic optimal control is to maximize a *gain* function over all admissible control  
 131 laws. In the discrete-time setting, this is given by the sum of the partial rewards  $F_t : \mathcal{X}_t \times \mathcal{U}_t \rightarrow \mathbb{R}$   
 132 for  $t = 0, \dots, T-1$ , and the terminal reward  $\Phi = F_T : \mathcal{X}_T \rightarrow \mathbb{R}$ . Then, we define the optimal  
 133 value function  $V_t : \mathcal{X}_t \rightarrow \mathbb{R}$  at time  $t$  as

$$134 \quad V_t := \sup_{u \in \mathcal{U}} \mathbb{E} \left[ \sum_{s=t}^{T-1} F_s(X_s^u, u_s(X_s^u)) + \Phi(X_T^u) \mid X_t^u \right]. \\ 135 \quad (5)$$

137 We now introduce the Bellman operator at time  $t$  as

$$138 \quad \mathcal{T}_t f(x) := \text{ess sup}_{u \in \mathcal{U}_t} F_t(x, u) + P_t^u f(x). \\ 139 \quad (6)$$

140 Bellman's principle (Bellman, 1966) implies that the optimal value function solves the dynamic  
 141 programming equation (Bertsekas & Shreve, 1996; Kallsen, 2016)

$$142 \quad \begin{cases} V_T(x) = \Phi(x), \\ V_t(x) = \mathcal{T}_t V_{t+1}(x), \quad t \in \{0, \dots, T-1\}. \end{cases} \\ 143 \quad (7)$$

145 We now want to represent Eq. 7 as a functional dynamic programming equation in some appropriate  
 146  $L^2$  spaces. To this end, we fix an auxiliary admissible control law  $\bar{u}$ , often called the behavior  
 147 policy in the RL literature (Sutton et al., 1998), and let  $\mu_t$  denote the distribution of  $X_t^{\bar{u}}$  on  $\mathcal{X}_t$ .  
 148 We introduce the following assumption to ensure that, if  $\Phi \in L_{\mu_T}^2$ , then the optimal value function  
 149 satisfying the dynamic system 7 belongs to  $L_{\mu_t}^2$  for all  $t \in \{0, \dots, T\}$ .

150 **Assumption 1** (Square integrability). *There exist constants  $c_F > 0$  and  $c_P > 0$  such that, for all  
 151  $t \in \{0, \dots, T\}$ :*

$$152 \quad \left\| \text{ess sup}_{u \in \mathcal{U}_t} |F_t(\cdot, u)| \right\|_{L_{\mu_t}^2} \leq c_F, \quad \left\| \text{ess sup}_{u \in \mathcal{U}_t} |P_t^u g| \right\|_{L_{\mu_t}^2} \leq c_P^{1/2} \|g\|_{L_{\mu_{t+1}}^2}, \\ 153 \quad (8)$$

155 for all  $g \in L_{\mu_{t+1}}^2$ . We further assume  $\Phi \in L_{\mu_T}^2$ .

157 Under these conditions,  $\mathcal{T}_t : L_{\mu_{t+1}}^2 \rightarrow L_{\mu_t}^2$ , see Lemma 2 in Appendix A for the complete proof.  
 158 Then  $V_t \in L_{\mu_t}^2$  for all  $t = \{0, \dots, T\}$ , and the dynamic programming problem 7 holds in each  
 159 corresponding  $L_{\mu_t}^2$  space. Further details on this assumption are discussed in Appendix D.

161 The main goal in the following will be to find a good estimate of the optimal value function at the  
 162 initial time  $t = 0$ , i.e.  $V_0$ , by leveraging the recursive formulation in 7.

162 **Example 1** (American Options). An American option is a financial contract that gives the holder  
 163 the right, but not the obligation, to buy or sell an underlying asset at a specified strike price at any  
 164 time up to the expiration date.

165 Let  $X$  be an exogenous Markov process, i.e., it is not influenced by any control variable or decision.  
 166 Let  $Q_t = Q_t(x, dx')$  denote its Markov transition kernel from  $\mathcal{X}_t$  to  $\mathcal{X}_{t+1}$ , which specifies the  
 167 conditional distribution of the next state  $X_{t+1}$  given the current state  $X_t = x$ . Suppose the underlying  
 168 asset has a price at time  $t$  given by a function  $S_t(X_t)$ . An American (call) option with strike  $K$  pays

$$C_t(X_t) = (S_t(X_t) - K)^+ \quad (9)$$

171 if exercised at time  $t$ . In practice, the dimension of the state space can be very high. For instance,  
 172  $S_t(X_t)$  could represent the maximum price in a basket of assets at time  $t$ , as in a so-called American  
 173 max-call option.

174 The holder of the American option aims to maximize the expected payoff  $\mathbb{E}[C_\tau(X_\tau)]$  over all exercise  
 175 strategies, i.e., over all stopping times  $\tau$ . We now cast this problem as a stochastic optimal control  
 176 problem 7. To this end, we introduce a cemetery state  $\Delta_\dagger \notin \mathcal{X}_t$  and define the augmented state space  
 177  $\mathcal{X}_t^{\Delta_\dagger} := \mathcal{X}_t \cup \{\Delta_\dagger\}$ . Any measurable function  $f$  on  $\mathcal{X}_t$  is extended to  $\mathcal{X}_t^{\Delta_\dagger}$  by setting  $f(\Delta_\dagger) := 0$ .  
 178 This is a standard technique in the theory of Markov processes, see Revuz & Yor (2013).

179 Define now the control space as  $\mathcal{U}_t := \{0, 1\}$ , where  $u = 0$  represents exercising the option and  
 180  $u = 1$  holding it. The controlled Markov transition kernel  $P_t^u$  is given by:

$$P_t^u(x, A) = \begin{cases} Q_t(x, A \cap \mathcal{X}_{t+1}) & \text{if } u = 1, x \in \mathcal{X}_t, \\ \delta_{\Delta_\dagger}(A) & \text{otherwise,} \end{cases}$$

184 for  $A \in \mathcal{B}(\mathcal{X}_{t+1}^\Delta)$ , meaning that the controlled process  $X_t^u$  follows the exogenous dynamics until the  
 185 option is exercised, after which it is absorbed in the state  $\Delta_\dagger$ . Define also:

$$F_t(\cdot, 1) = 0, \quad F_t(\cdot, 0) = C_t, \quad \Phi = C_T. \quad (10)$$

188 An admissible control law  $u$  then consists of measurable functions  $u_t : \mathcal{X}_t^{\Delta_\dagger} \rightarrow \{0, 1\}$ , with the  
 189 convention  $u_t(\Delta_\dagger) = 0$ . The associated exercise strategy is defined by:

$$\tau := \inf\{t \mid u_t = 1\} \wedge T, \quad (11)$$

192 i.e., the first time  $t \in \{0, \dots, T-1\}$  such that  $u_t = 0$ , or  $T$  if no such time exists (with  $\inf \emptyset = \infty$ ).  
 193 The dynamic programming problem 7 then becomes:

$$\begin{cases} V_T(x) = C_T(x), \\ V_t(x) = \max \{C_t(x), e^{-r} Q_t V_{t+1}(x)\}, \end{cases} \quad (12)$$

197 which selects the maximum between the immediate exercise value and the (discounted) continuation  
 198 value. Here,  $r$  denotes the risk-free interest rate.

### 200 3 SAMPLE-BASED VALUE FUNCTION APPROXIMATION

202 Stochastic dynamic control problem 7 is not directly solvable in practice, primarily because we do  
 203 not have access to the true expectation in  $P_t^u$ . A standard way to address this issue is to approximate  
 204 the expectation via Monte Carlo simulation. Let  $\{z_i^{(t+1)}\}_{i=1}^{M_t} \sim \mathbb{P}_{t+1}^{M_t}$  be i.i.d. samples from the  
 205 distribution of the stochastic driver  $Z_{t+1}$ . We then define

$$\widetilde{P}_t^u f(x) := \frac{1}{M_t} \sum_{i=1}^{M_t} f(\pi_t(x, u, z_i^{(t+1)})), \quad \widetilde{T}_t f(x) := \text{ess sup}_{u \in \mathcal{U}_t} \{F_t(x, u) + \widetilde{P}_t^u f(x)\}, \quad (13)$$

210 the empirical approximation of  $P_t^u$  and the associated empirical Bellman operator, respectively.  
 211 By the Law of Large Numbers and the Continuous Mapping Theorem, we obtain:

$$\widetilde{P}_t^u f(x) \xrightarrow{a.s.} P_t^u f(x), \quad \widetilde{T}_t f(x) \xrightarrow{a.s.} T_t f(x), \quad \text{for } M_t \rightarrow \infty. \quad (14)$$

214 However, a naive application of this approximation—by recursively replacing  $P_t^u$  with  $\widetilde{P}_t^u$  in the dy-  
 215 namic programming equation—fails in practice, resulting in a nested Monte Carlo procedure whose

computational cost grows exponentially with  $T$ , making it infeasible for large time horizons. To mitigate this, we adopt a more efficient approach: we proceed backward in time and use regression to construct a sequence of function approximators for each  $V_t$ . At each stage, we generate samples and solve a supervised learning problem, leveraging the approximation of  $V_{t+1}$  obtained in the previous step (with the terminal condition  $V_T = \Phi$  known a priori). Specifically, assume we have already computed an approximation of  $V_{t+1}$ , denoted by  $\widehat{W}_{t+1}^{\lambda_{t+1}}$  (this  $\widehat{\cdot}$  notation will be explained below in Eq. 18). We then generate training data  $\{(x_i, y_i)\}_{i=1}^{n_t}$ , where  $x_i \sim \mu_t$  and

$$y_i = \widetilde{\mathcal{T}}_t \widehat{W}_{t+1}^{\lambda_{t+1}}(x_i). \quad (15)$$

We now solve the corresponding regression problem using a suitable supervised learning method. A classical choice is *regularized empirical risk minimization* (ERM) with Tikhonov regularization. Combined with kernel methods, and with the natural choice of the square loss as the loss function, this yields the well-known *Kernel Ridge Regression* (KRR).

**Assumption 2** (Reproducing Kernel Hilbert Space). *Let  $\mathcal{H}_k$  be a separable reproducing kernel Hilbert space (RKHS) of real-valued functions on  $\mathcal{X}$ , with inner product  $\langle \cdot, \cdot \rangle_{\mathcal{H}_k}$  and associated norm  $\|\cdot\|_{\mathcal{H}_k}$ . Let  $k : \mathcal{X} \times \mathcal{X} \rightarrow \mathbb{R}$  be the reproducing kernel of  $\mathcal{H}_k$  and assume it is bounded, i.e., there exists  $\kappa > 0$  such that  $\sup_{x \in \mathcal{X}} k(x, x) \leq \kappa^2$ .*

**Remark 2.** *Although we use standard well-spread Monte Carlo sampling in this step, this is not the only viable choice. Any quadrature rule (e.g., monomial rules) can be used in place of Eq. 13 to approximate the operator  $P_t^u$ . This flexibility can be especially valuable in high-dimensional settings or when Monte Carlo sampling error is non-negligible, as some quadrature methods may achieve much higher precision using fewer points.*

**KRR estimator.** For a regularization parameter  $\lambda_t > 0$ , the KRR estimator at time  $t$  is defined as

$$\widehat{W}_t^{\lambda_t} := \arg \min_{f \in \mathcal{H}_k} \frac{1}{n_t} \sum_{i=1}^{n_t} (y_i - f(x_i))^2 + \lambda_t \|f\|_{\mathcal{H}_k}^2 \quad (16)$$

Note that at maturity, the value function  $V_T$  is known and equals  $\Phi$ , so no approximation is needed at the final step. Also note that, given Eq. 15,  $\widetilde{\mathcal{T}}_t \widehat{W}_{t+1}^{\lambda_{t+1}}$  is the regression target function, i.e.,

$$W_t^* := \widetilde{\mathcal{T}}_t \widehat{W}_{t+1}^{\lambda_{t+1}} = \arg \min_{f \in L_{\mu_t}^2} \mathbb{E}[(Y - f(X))^2] = \arg \min_{f \in L_{\mu_t}^2} \mathbb{E}[(\widetilde{\mathcal{T}}_t \widehat{W}_{t+1}^{\lambda_{t+1}}(X) - f(X))^2] \quad (17)$$

since  $\widetilde{\mathcal{T}}_t \widehat{W}_{t+1}^{\lambda_{t+1}} \in L_{\mu_t}^2$  under Assumption 1. In general,  $W_t^* \notin \mathcal{H}_k$ , i.e. the model is misspecified. We will mention this further in the next section when introducing the well-known *source condition*.

Before turning to the statistical analysis, we introduce a refinement of our estimator, which also justifies the notation  $\widehat{\cdot}$  used above. This step will be important to control approximation errors in the next section. We recall the following definitions, see Chapter 6 in Steinwart & Christmann (2008a). Given a threshold parameter  $B > 0$ , we define the *clipped* version of  $a \in \mathbb{R}$  as:

$$\widehat{a} := \min\{\max\{a, -B\}, B\}. \quad (18)$$

We say that a loss function  $\ell$  is *clippable* at level  $B > 0$  if for all  $y \in \mathcal{Y}$  and  $a \in \mathbb{R}$ ,  $\ell(y, \widehat{a}) \leq \ell(y, a)$ . It is easy to verify that many loss functions are clippable. In particular, the square loss (which we use) can be clipped at  $B$  when the output  $y \in [-B, B]$ . Note that if  $Y$  is generated as in Eq. 15, a sufficient condition for boundedness is  $\sup_{x \in \mathcal{X}_t, u \in \mathcal{U}_t} |F_t(x, u)| < B$ . In practice,  $F_t(x, u)$  is often unbounded (e.g., option payoffs), but boundedness can be enforced without loss of rigor by restricting the dynamics to a compact subset of the state space. In financial applications, for instance,  $\mu_t$  is typically induced by a discretized geometric Brownian motion, hence log-normal with exponentially decaying tails. Consequently, large deviations of  $X_t$  are extremely rare, and truncation introduces only negligible error while allowing the use of the clipped estimator  $\widehat{W}_t^{\lambda_t}$ , as required in Steinwart & Christmann (2008b).

The resulting method—that for simplicity we will indicate as KRR-DP (Kernel Ridge Regression-Dynamic Programming) in the following—is summarized in Algorithm 1.

**Example 2** (American Options (cont.)). *We now return to the American options application introduced in Example 1, and continue adapting our model to this setting. Here, the state vector*

270  $X_t = (X_t^1, \dots, X_t^d)^\top \in \mathbb{R}_+^d$  represents the prices of  $d$  underlying assets at time  $t$ . A common model  
 271 for their evolution is geometric Brownian motion (GBM), whose dynamics are given by  
 272

$$273 \quad dX_t^i = rX_t^i dt + \sigma_i X_t^i (\rho^{1/2} dB_t)^i, \quad (19)$$

274 for  $i = 1, \dots, d$ , with  $r \in \mathbb{R}$  the risk-free rate,  $\sigma_i > 0$  the volatility of asset  $i$ ,  $\rho \in \mathbb{R}^{d \times d}$  the  
 275 correlation matrix and  $B_t = (B_t^1, \dots, B_t^d)^\top$  a  $d$ -dimensional Brownian motion with independent  
 276 components. We consider discrete times  $t = 0, \dots, T$  and approximate the dynamics with  
 277

$$278 \quad X_{t+1}^i = X_t^i \cdot \exp \left( \left( r - \frac{1}{2} \sigma_i^2 \right) + \sigma_i (\rho^{1/2} z)_i \right), \quad (20)$$

279 where  $z = (z_1, \dots, z_d)^\top \sim \mathcal{N}(0, I_d)$  is a vector of independent standard Gaussian variables.  
 280 As an example, we define a max-call option with strike price  $K > 0$ , for which  $S_t(X_t) =$   
 281  $\max\{X_t^1, \dots, X_t^d\}$ , and the payoff at time  $t$  is given by  
 282

$$283 \quad C_t(X_t) = (S_t(X_t) - K)^+ = \left( \max_{1 \leq i \leq d} X_t^i - K \right)^+. \quad (21)$$

284 The transition function  $\pi_t : \mathbb{R}_+^d \times \mathcal{U}_t \times \mathbb{R}^d \rightarrow \mathbb{R}_+^d$  is defined as  
 285

$$286 \quad \pi_t(x, u, z) := \begin{cases} \Delta^\dagger & \text{if } u = 0, \\ x \odot \exp \left( \left( r - \frac{1}{2} \sigma^2 \right) + \sigma \odot (\rho^{1/2} z) \right) & \text{otherwise,} \end{cases}$$

287 with  $\sigma = (\sigma_1, \dots, \sigma_d)^\top$ ,  $\odot$  the elementwise multiplication.  
 288

---

289 **Algorithm 1:** KRR-DP for American Option Pricing (backward induction with MC + KRR)

---

290 **Inputs:**  $T; r; \{C_t, \mu_t, \pi_t, n_t, M_t\}_{t=0}^{T-1}$ ; KRR hyperparameters  $\{\Theta_t\}_{t=0}^{T-1}$  (kernel,  $\lambda_t$ , etc.).  
 291 **Output:** Estimator  $\widehat{W}_0^{\lambda_0} : \mathbb{R}^d \rightarrow \mathbb{R}$  of the value of the option  $V_0$ .  
 292 // MC estimate of discounted continuation under ‘‘hold’’ ( $u = 1$ )  
 293  
 1 **Function** ContinuationValue( $x, M_t, \pi_t, \widehat{W}_{t+1}^{\lambda_{t+1}}$ ):  
 2   | Sample  $z^{(1)}, \dots, z^{(M_t)}$  i.i.d.  $\mathbb{P}_{t+1}$ ; // e.g.,  $z \sim \mathcal{N}(0, I)$   
 3   | **for**  $j = 1, \dots, M_t$  **do**  
 4   | |  $\tilde{x}_j \leftarrow \pi_t(x, u=1, z^{(j)})$ ;  
 5   | **end**  
 6   | **return**  $e^{-r\Delta t} \frac{1}{M_t} \sum_{j=1}^{M_t} \widehat{W}_{t+1}^{\lambda_{t+1}}(\tilde{x}_j)$ ;  
 7   // Generate supervised data  $(\widehat{X}_t, \widehat{y}_t)$  at stage  $t$   
 8   | **Function** DataGeneration( $n_t, M_t, \mu_t, \pi_t, C_t, \widehat{W}_{t+1}^{\lambda_{t+1}}$ ):  
 9   | | Sample  $\widehat{X}_t = [x_1, \dots, x_{n_t}]^\top$ , with  $x_i \stackrel{\text{i.i.d.}}{\sim} \mu_t$ ;  
 10   | | **parallel for**  $i = 1, \dots, n_t$  **do**  
 11   | | |  $q_i \leftarrow \text{ContinuationValue}(x_i, M_t, \pi_t, \widehat{W}_{t+1}^{\lambda_{t+1}})$ ; // MC continuation  
 12   | | |  $y_i \leftarrow \max(C_t(x_i), q_i)$ ; // Bellman: exercise vs. continue  
 13   | | **end**  
 14   | | **return**  $(\widehat{X}_t, \widehat{y}_t = [y_1, \dots, y_{n_t}]^\top)$   
 15   // Main backward pass  
 16   | **Function** OptionPricing( $\{(n_t, M_t, \mu_t, \pi_t, C_t, \Theta_t)\}_{t=0}^T$ ):  
 17   | |  $\widehat{W}_T^{\lambda_T} \leftarrow C_T \equiv \Phi$ ; // terminal value is known  
 18   | | **for**  $t = T-1, \dots, 0$  **do**  
 19   | | |  $(\widehat{X}_t, \widehat{y}_t) \leftarrow \text{DataGeneration}(n_t, M_t, \mu_t, \pi_t, C_t, \widehat{W}_{t+1}^{\lambda_{t+1}})$ ;  
 20   | | |  $\widehat{W}_t^{\lambda_t} \leftarrow \text{Regression}((\widehat{X}_t, \widehat{y}_t), \Theta_t)$ ; // KRR/FALKON on  $(\widehat{X}_t, \widehat{y}_t)$   
 21   | | **end**  
 22   | | **return**  $\widehat{W}_0^{\lambda_0}$

---

324 **4 ERROR ANALYSIS AND BACKWARD PROPAGATION**  
 325

326 In this section, our primary goal is to provide theoretical guarantees for our estimator  $\widehat{W}_t^{\lambda_t}$  and to  
 327 study how the error propagates backward in time from  $T$  to 0. In particular, we are interested in  
 328 analyzing the rate of convergence of  $\widehat{W}_t^{\lambda_t}$  to the target value function  $V_t$  in some norm, as a function  
 329 of the sample sizes  $n_t$  and  $M_t$ . A natural choice is to bound  
 330

331 
$$\mathcal{E}_t = \|\widehat{W}_t^{\lambda_t} - V_t\|_{L_{\mu_t}^2}^2. \quad (22)$$
  
 332

333 **4.1 ERROR DECOMPOSITION**  
 334

335 To do so, we split the total error into three components:  
 336

337 
$$\mathcal{E}_t \lesssim \|\widehat{W}_t^{\lambda_t} - \widetilde{\mathcal{T}}_t \widehat{W}_{t+1}^{\lambda_{t+1}}\|_{L_{\mu_t}^2}^2 + \|\widetilde{\mathcal{T}}_t \widehat{W}_{t+1}^{\lambda_{t+1}} - \mathcal{T}_t \widehat{W}_{t+1}^{\lambda_{t+1}}\|_{L_{\mu_t}^2}^2 + \|\mathcal{T}_t \widehat{W}_{t+1}^{\lambda_{t+1}} - \mathcal{T}_t V_{t+1}\|_{L_{\mu_t}^2}^2. \quad (23)$$
  
 338

339 Notice that the rigorous mathematical formulation established above ensures the well-definedness  
 340 of all terms, allowing us to meaningfully leverage this structure to decompose the total error. The  
 341 resulting splitting is a key advantage of our framework: the error separates into three distinct com-  
 342 ponents, each associated with a different approximation step. Because the bound is fully modular,  
 343 each term can be improved independently without affecting the rest of the analysis.

344 Term I depends only on the regression method—while we use kernel ridge regression for its clear  
 345 statistical guarantees, other function approximators (e.g., neural networks) could be substituted.  
 346 Term II isolates the sampling error, so Monte Carlo can be replaced by more refined schemes such  
 347 as quadrature or variance-reduced estimators. Term III captures the intrinsic propagation induced  
 348 by the dynamics and is unaffected by choices in the first two terms. This flexible structure allows us  
 349 to work on each component independently while preserving the overall analysis.

350 **Term I: Regression Error.** The first term is the standard machine learning error due to the fact  
 351 that our estimator minimizes the empirical risk in Eq. 16, based only on a finite sample  $\{(x_i, y_i)\}_{i=1}^{n_t}$ .  
 352 Our target is the regression function  $W_t^* = \widetilde{\mathcal{T}}_t \widehat{W}_{t+1}^{\lambda_{t+1}}$ , as defined in Eq. 17. Term I then corresponds  
 353 to the so-called excess risk of  $\widehat{W}_t^{\lambda_t}$ :

355 
$$\mathcal{R}(\widehat{W}_t^{\lambda_t}) - \mathcal{R}(W_t^*) := \mathbb{E} [(Y - \widehat{W}_t^{\lambda_t}(X))^2 - (Y - W_t^*(X))^2] = \|\widehat{W}_t^{\lambda_t} - W_t^*\|_{L_{\mu_t}^2}^2, \quad (24)$$
  
 356

357 (see Caponnetto & De Vito (2007)), where  $\mathcal{R}(\widehat{W}_t^{\lambda_t})$  is the risk of  $\widehat{W}_t^{\lambda_t}$  and  $\mathcal{R}(W_t^*) = \mathcal{R}(\widetilde{\mathcal{T}}_t \widehat{W}_{t+1}^{\lambda_{t+1}})$ .  
 358 It represents the expected error of our estimator on new data compared to the regression function.  
 359

360 We introduce the following regularity assumption, commonly referred to as the *source condition*.

361 **Assumption 3** (Source Condition). *There exists  $\beta_t \in (0, 1]$  such that  $W_t^* \in L_k^{\beta_t/2}(L_{\mu_t}^2)$ , where*  
 362  *$L_k : L_{\mu_t}^2 \rightarrow L_{\mu_t}^2$  is the integral operator associated with the kernel  $k$ .*  
 363

364 Assumption 3 and equivalent formulations (e.g., Assumption 4 in Rudi et al. (2015a)) are standard  
 365 in the literature (Smale & Zhou, 2007; Caponnetto & De Vito, 2007). The parameter  $\beta_t$  quantifies  
 366 the smoothness of the target function  $W_t^*$  and how well it can be approximated by elements in  $\mathcal{H}_k$ .  
 367 When  $\beta_t = 1$ , we are in the *well-specified* setting, i.e.,  $W_t^* \in \mathcal{H}_k$ . Our main focus, however, is on  
 368 the *misspecified* setting with  $\beta_t < 1$ , where  $W_t^* \notin \mathcal{H}_k$ .

369 Under the square loss, Assumption 3 is directly related to the approximation error, as shown in Smale  
 370 & Zhou (2003); Steinwart et al. (2009). Using a result from Corollary 6 in Steinwart et al. (2009)  
 371 (see Appendix B.1), we obtain the following upper bound in terms of  $n_t$ : choosing  $\lambda_t \sim n_t^{-\frac{1}{\beta_t+1}}$ ,  
 372 with high probability,

373 
$$\|\widehat{W}_t^{\lambda_t} - \widetilde{\mathcal{T}}_t \widehat{W}_{t+1}^{\lambda_{t+1}}\|_{L_{\mu_t}^2}^2 \lesssim n_t^{-\frac{\beta_t}{\beta_t+1}}. \quad (25)$$
  
 374

375 We refer to Appendix B.1 for further details. Note that the above rate can be made faster by assuming  
 376 some polynomial (or even exponential) decay of the spectrum of the integral operator  $L_k$ . This is  
 377 deeply connected to the well-known *capacity assumption*, which for simplicity is not assumed here  
 in the main text. Further details and the resulting faster rate can be found in Appendix B.1.

378 **Term II: Monte Carlo Error.** The second term accounts for the Monte Carlo error introduced  
 379 when approximating the unknown expectation in  $\mathcal{T}_t$ , as discussed in Section 3.

380 Using the definitions of  $\mathcal{T}_t$  and  $\widetilde{\mathcal{T}}_t$  from Eqs. 6 and 13, together with Lemma 1 in Appendix A, and  
 381 denoting  $\mathcal{F}_t^x = \{z \mapsto \widehat{W}_{t+1}^{\lambda_{t+1}}(\pi_t(x, u, z)) : u \in \mathcal{U}_t\}$ , we obtain that, with high probability,  
 382

$$383 \quad \|\widetilde{\mathcal{T}}_t \widehat{W}_{t+1}^{\lambda_{t+1}} - \mathcal{T}_t \widehat{W}_{t+1}^{\lambda_{t+1}}\|_{L_{\mu_t}^2}^2 \leq \left\| \sup_{f \in \mathcal{F}_t^x} \left| \frac{1}{M_t} \sum_{j=1}^{M_t} f(z_j) - \mathbb{E}[f(Z_{t+1})] \right| \right\|_{L_{\mu_t}^2}^2 \lesssim \left\| \mathbb{E} \widehat{\mathcal{R}}(\mathcal{F}_t^x) + \sqrt{\frac{1}{M_t}} \right\|_{L_{\mu_t}^2}^2$$

387 where the last inequality follows from the boundedness of  $\widehat{W}_{t+1}^{\lambda_{t+1}}$  and an application of Boucheron  
 388 et al. (2005, Theorem 3.2), while  $\widehat{\mathcal{R}}(\mathcal{F}_t^x)$  denotes the well-known empirical Rademacher complexity  
 389 of  $\mathcal{F}_t^x$  (see definition in Appendix B.2). Bounding such complexities is a classical problem in  
 390 statistical learning theory (Bartlett & Mendelson, 2002). In our setting, we focus on two relevant  
 391 cases: (i) finite classes, as in American options where the control set is binary ( $\mathcal{U}_t = \{0, 1\}$ ), and  
 392 (ii) Lipschitz transitions  $\pi_t$ , which are typical in financial models once the state space is a compact  
 393 set (see the discussion about truncation in previous section). Using results from Massart (2000);  
 394 Bartlett & Mendelson (2002) (see Appendix B.2), we obtain for both cases

$$395 \quad \mathbb{E} \widehat{\mathcal{R}}(\mathcal{F}_t^x) \lesssim \sqrt{1/M_t}. \quad (26)$$

398 **Term III: Propagation Error.** This term captures the error inherited from the previous step  $t + 1$ .  
 399 By Lemma 2 in Appendix A, we have:

$$400 \quad \|\mathcal{T}_t \widehat{W}_{t+1}^{\lambda_{t+1}} - \mathcal{T}_t V_{t+1}\|_{L_{\mu_t}^2}^2 \leq c_P \|\widehat{W}_{t+1}^{\lambda_{t+1}} - V_{t+1}\|_{L_{\mu_t}^2}^2 = c_P \mathcal{E}_{t+1}.$$

403 **Final Bound.** Putting everything together, we obtain the following result.

404 **Theorem 1** (Error Backpropagation). *Under Assumptions 1, 2, 3, and provided that condition 26  
 405 holds, with the choice  $\lambda_t \sim n_t^{-\frac{1}{\beta_t+1}}$  and  $M_t \sim n_t^{\frac{\beta_t}{\beta_t+1}}$ , we have with high probability:*

$$406 \quad \mathcal{E}_t = \|\widehat{W}_t^{\lambda_t} - V_t\|_{L_{\mu_t}^2}^2 \lesssim \left( \frac{1}{n_t} \right)^{\frac{\beta_t}{\beta_t+1}} + c_P \mathcal{E}_{t+1}, \quad (27)$$

410 for  $t \in \{0, \dots, T-1\}$ . Furthermore,

$$412 \quad \mathcal{E}_0 = \|\widehat{W}_0^{\lambda_0} - V_0\|_{L_{\mu_0}^2}^2 \lesssim \sum_{t=0}^{T-1} c_P^t \left( \frac{1}{n_t} \right)^{\frac{\beta_t}{\beta_t+1}}. \quad (28)$$

415 Note that, as desirable, the error vanishes as  $n_t \rightarrow \infty$  for all  $t$ . In the non-asymptotic regime, the  
 416 convergence rate depends on the smoothness parameters  $\{\beta_t\}_t$ , which reflect the level of misspeci-  
 417 fication of the problem. Although the expectation operator  $\widetilde{P}_t^u$  may act as a smoothing operator, the  
 418 supremum in the Bellman operator prevents us from guaranteeing a smoothing effect through time.  
 419 As a result, the problem generally remains misspecified throughout the backward recursion. Note  
 420 also that the constant  $c_P$  in Assumption 1 plays a key role in controlling the resulting error propa-  
 421 gation. When  $c_P < 1$ , as in our option pricing setting (see Example 3 below), the recursion becomes  
 422 contractive, so errors are damped rather than amplified, making convergence faster and more stable.

423 **Example 3** (American Options (cont.)). *Returning to our application to American option pricing  
 424 in Example 1, we now adapt Theorem 1 to this setting. Note that  $W_T^* = V_T = \Psi$  is typically non-  
 425 smooth for common payoff functions, see Eq. 9 or Fig. 1-2 in Appendix C). As mentioned above,  
 426 this places us in the misspecified case, where the smoothness parameters  $\{\beta_t\}_t$  can be small, while  
 427 it is not clear if the specification eventually improves throughout the recursion. From Eq. 12, the  
 428 Bellman operator  $\mathcal{T}_t : L_{\mu_{t+1}}^2 \rightarrow L_{\mu_t}^2$  takes the form:*

$$429 \quad \mathcal{T}_t g = \max(C_t, e^{-r} Q_t g). \quad (29)$$

431 We now verify that the assumptions required by Theorem 1 are satisfied. First condition in  
 432 Eq. 8 in Assumption 1 is straightforward since  $U_t = \{0, 1\}$  and  $F_t$  is defined as in Eq. 10:

432

433

Table 1: Results for a Geometric basket Put option, see Table 1 in Goudenege et al. (2020).

434

435

		KRR-DP		GPR-Tree		GPR-EI		Ekvall	Benchmark
$d$	Price	95% CI	Time	Price	Time	Price	Time	Price	Price
2	4.63	[4.58, 4.68]	2s	4.61	22s	4.57	26s	4.62	4.62
5	3.46	[3.42, 3.50]	3s	3.44	23s	3.41	27s	3.44	3.45
10	2.98	[2.94, 3.03]	4s	2.93	60s	2.93	30s	2.90	2.97
20	2.70	[2.68, 2.72]	21s	2.72	49609s	2.63	29s	2.70	2.70
40	2.55	[2.53, 2.57]	87s	/	/	2.53	38s	2.57	2.56

441

442

443

Table 2: Results for a Max-Call option, see Table 3 in Goudenege et al. (2020).

444

		KRR-DP		GPR-Tree		GPR-EI		GPR-MC	Ekvall
$d$	Price	95% CI	Time	Price	Time	Price	Time	Price	Price
2	16.93	[16.86, 17.00]	5s	16.93	20s	16.82	28s	16.86	16.86
5	27.16	[26.98, 27.33]	5s	27.19	26s	26.95	27s	27.20	27.20
10	35.14	[34.94, 35.35]	6s	35.08	106s	34.84	29s	35.17	/
20	42.62	[42.30, 42.93]	27s	43.00	51090s	42.62	35s	42.76	/
40	50.44	[50.01, 50.87]	118s	/	/	49.53	41s	50.70	/

451

452

ess sup $_{u \in \{0,1\}}$   $|F_t(\cdot, u)| = F_t(\cdot, 0) = C_t$ . We let  $c_F$  be the squared  $L^2_{\mu_t}$ -norm of  $C_t$ , which is assumed to be finite. Moreover, since  $Q_t$  is a Markov transition kernel, it defines a non-expansive operator:

456

$$\|Q_t g\|_{L^2_{\mu_t}}^2 = \int_{\mathcal{X}_t} \left( \int_{\mathcal{X}_{t+1}} g(x') Q(x, dx') \right)^2 d\mu_t \leq \int_{\mathcal{X}_{t+1}} g(x')^2 \int_{\mathcal{X}_t} Q(x, dx') d\mu_t \leq \|g\|_{L^2_{\mu_{t+1}}}^2,$$

459

460

where we used Jensen's inequality and Fubini's theorem. Therefore, condition 8 in Assumption 1 is also satisfied. We can now bound the Bellman operator  $\mathcal{T}_t$ :

461

462

$$\|\mathcal{T}_t g\|_{L^2_{\mu_t}} = \|\max(C_t, e^{-r} Q_t g)\|_{L^2_{\mu_t}} \leq c_F + e^{-r} \|g\|_{L^2_{\mu_{t+1}}} \quad (30)$$

463

464

Then, Assumption 1 is satisfied with  $c_P = e^{-2r}$ . Note also that  $c_P < 1$  in the common case of a strictly positive risk-free interest rate  $r$ .

466

467

**Corollary 1** (American Option Pricing). *From Theorem 1, in the setting described in Example 1, 2 and 3, and following Algorithm 1, we have with high probability:*

468

469

$$\|\widehat{W}_0^{\lambda_0} - V_0\|_{L^2_{\mu_0}}^2 \lesssim \sum_{t=0}^{T-1} e^{-rt} \left( \frac{1}{n_t} \right)^{\frac{\beta_t}{\beta_t+1}}. \quad (31)$$

470

471

Notice that, in the common case of a positive interest rate  $e^{-rt} < 1$  (i.e.  $c_P < 1$ ), the Bellman operator is contractive in this setting. This contraction plays a crucial role in the corollary: it damps the propagated errors across time steps, thereby facilitating convergence of the overall approximation.

475

476

## 5 SIMULATIONS

477

478

In this section, we present a basic implementation of KRR-DP Algorithm 1 and conduct an initial evaluation of the effectiveness of the proposed method. More comprehensive experiments and optimized implementations will be the subject of future work.

481

482

483

484

485

We primarily compare our results with the numerical benchmarks reported in Goudenege et al. (2020). Specifically, we replicate the results in their Table 1 and Table 3, which correspond to pricing a geometric basket put option and a max-call option, respectively. Note that a theoretical benchmark exists for geometric basket put options. The parameters are set reproducing the ones in Goudenege et al. (2020) and are the following: time horizon  $T = 9$ , initial state  $X_0^i = 100$  for  $1 \leq i \leq d$ , strike price  $K = 100$ , free-risk interest rate  $r = 0.05$ , volatility  $\sigma_i = 0.2$  for  $1 \leq i \leq d$ ,

486 and correlation  $\rho_{ij} = 0.2$  for  $1 \leq i \neq j \leq d$ .

487 As regards the KRR solver, we employ the efficient FALKON algorithm (Meanti et al., 2020), which  
 488 uses Nyström-based random projections (Williams & Seeger, 2000) to achieve substantial compu-  
 489 tational savings while retaining optimal statistical performance (Rudi et al., 2015b; Della Vecchia  
 490 et al., 2021; 2024). Importantly, FALKON is fully compatible with our theoretical analysis: its  
 491 Nyström approximation enjoys provably optimal excess-risk guarantees (given a sufficient number  
 492 of centers), and thus can directly replace the full KRR estimator in Term I of our error decomposi-  
 493 tion (see Section 6 in Della Vecchia et al. (2024)). Thanks to the modular structure of our bounds,  
 494 this substitution preserves the convergence rate in Eq. (25), does not affect the other terms, and  
 495 leaves the overall propagation rate in Eq. (28) unchanged—while significantly reducing computa-  
 496 tional cost. This illustrates a key advantage of the neat and transparent structure of our framework:  
 497 each source of error can be improved independently (e.g., by refining Monte Carlo or replacing it  
 498 with more efficient quadrature) without altering the overall analysis. A description of the involved  
 499 methods and further details on our simulations are given in Appendix C.

500 These preliminary results suggest that our method performs competitively in this setting with the  
 501 considered benchmarks, offering a favorable trade-off between accuracy and computational effi-  
 502 ciency. As the dimension increases, however, the runtime grows noticeably, with the Monte Carlo  
 503 component (Term II) emerging as the main computational bottleneck. The study and incorporation  
 504 of alternatives to standard Monte Carlo capable of reducing the required number of samples  $M$  while  
 505 preserving statistical guarantees (such as the above-mentioned quadrature rules) will be the basis for  
 506 a competitive large-scale implementation, and constitute the natural direction for follow-up work.

## 507 6 CONCLUSIONS AND FUTURE WORK

509 In this work, we addressed stochastic optimal control problems in discrete time and introduced a  
 510 kernel-based regression framework for their solution. Our approach combines backward recursion  
 511 via empirical Bellman operators with Monte Carlo simulation and regularized learning techniques to  
 512 construct data-driven approximations of the value function. The framework is supported by rigorous  
 513 theoretical guarantees, including explicit error bounds.

514 Several promising directions remain open for future work. First, we plan to extend the prelim-  
 515 inary simulations presented above into a more comprehensive experimental study, incorporating  
 516 real-world datasets and more complex models. In particular, our framework can naturally be adapted  
 517 to other non-standard applications in economics, such as partial equilibrium, optimal consumption,  
 518 or goal-based investing.

519 In parallel, there is significant room to improve computational efficiency, especially in high-  
 520 dimensional settings, by developing a competitive implementation of the algorithm. While the  
 521 regression step can be accelerated, as in our simulations, using established scalability techniques  
 522 that preserve the statistical guarantees of KRR (e.g., sketching, random features, Nyström approxi-  
 523 mations), the main bottleneck in our pipeline appears to be the Monte Carlo data-generation step.  
 524 Reducing the number  $M$  of simulated points is critical for speeding up the DATAGENERATION func-  
 525 tion in Algorithm 1. A possible approach is to replace standard Monte Carlo sampling with more  
 526 sophisticated quadrature schemes (e.g., monomial rules), which may significantly reduce computa-  
 527 tional cost while maintaining accuracy.

## 528 REFERENCES

530 Lokman Abbas-Turki and Bernard Lapeyre. American options by malliavin calculus and nonpara-  
 531 metric variance and bias reduction methods. *SIAM Journal on Financial Mathematics*, 3(1):  
 532 479–510, 2012.

533 Leif Andersen and Mark Broadie. Primal-Dual Simulation Algorithm for Pricing Multidimensional  
 534 American Options. *Management Science*, 50(9):1222–1234, 2004. ISSN 0025-1909. URL <https://www.jstor.org/stable/30046229>. Publisher: INFORMS.

535 Karl J Åström. *Introduction to stochastic control theory*. Courier Corporation, 2012.

536 Vlad Bally, Gérard Pagès, and Jacques Printems. First-order schemes in the numerical quantization  
 537 method. *Mathematical Finance*, 13(1):1–16, 2003.

540 Vlad Bally, Lucia Caramellino, and Antonino Zanette. Pricing and hedging american options by  
 541 monte carlo methods using a malliavin calculus approach. *Monte Carlo Methods and Applica-*  
 542 *tions*, 11(2):97–133, 2005.

543

544 Peter L Bartlett and Shahar Mendelson. Rademacher and gaussian complexities: Risk bounds and  
 545 structural results. *Journal of Machine Learning Research*, 3(Nov):463–482, 2002.

546

547 Sebastian Becker, Patrick Cheridito, and Arnulf Jentzen. Deep optimal stopping. *Journal of Machine*  
 548 *Learning Research*, 20(74):1–25, 2019.

549

550 Richard Bellman. Dynamic programming. *science*, 153(3731):34–37, 1966.

551

552 Denis Belomestny, John Schoenmakers, and Fabian Dickmann. Multilevel dual approach for pricing  
 553 american style derivatives. *Finance and Stochastics*, 17:717–742, 2013.

554

555 Julius Berner, Lorenz Richter, and Karen Ullrich. An optimal control perspective on diffusion-based  
 556 generative modeling. *arXiv preprint arXiv:2211.01364*, 2022.

557

558 Dimitri Bertsekas. *Dynamic programming and optimal control: Volume I*, volume 4. Athena scien-  
 559 tific, 2012.

560

561 Dimitri Bertsekas and Steven E Shreve. *Stochastic optimal control: the discrete-time case*, volume 5.  
 562 Athena Scientific, 1996.

563

564 Bruno Bouchard and Nizar Touzi. Discrete-time approximation and monte-carlo simulation of back-  
 565 ward stochastic differential equations. *Stochastic Processes and their Applications*, 111(2):175–  
 566 206, 2004.

567

568 Stéphane Boucheron, Olivier Bousquet, and Gábor Lugosi. Theory of classification: A survey of  
 569 some recent advances. *ESAIM: probability and statistics*, 9:323–375, 2005.

570

571 Mark Broadie and Paul Glasserman. Pricing american-style securities using simulation. *Journal of*  
 572 *Economic Dynamics and Control*, 21(8-9):1323–1352, 1997.

573

574 Andrea Caponnetto and Ernesto De Vito. Optimal rates for the regularized least-squares algorithm.  
 575 *Foundations of Computational Mathematics*, 7:331–368, 2007.

576

577 René Carmona. *Lectures on BSDEs, stochastic control, and stochastic differential games with finan-*  
 578 *cial applications*. SIAM, 2016.

579

580 Pratik Chaudhari, Adam Oberman, Stanley Osher, Stefano Soatto, and Guillaume Carlier. Deep  
 581 relaxation: partial differential equations for optimizing deep neural networks. *Research in the*  
 582 *Mathematical Sciences*, 5:1–30, 2018.

583

584 Andrea Della Vecchia, Jaouad Mourtada, Ernesto De Vito, and Lorenzo Rosasco. Regularized erm  
 585 on random subspaces. In *International Conference on Artificial Intelligence and Statistics*, pp.  
 586 4006–4014. PMLR, 2021.

587

588 Andrea Della Vecchia, Ernesto De Vito, Jaouad Mourtada, and Lorenzo Rosasco. The nyström  
 589 method for convex loss functions. *Journal of Machine Learning Research*, 25(360):1–60, 2024.

590

591 Carles Domingo i Enrich, Jiequn Han, Brandon Amos, Joan Bruna, and Ricky TQ Chen. Stochas-  
 592 tic optimal control matching. *Advances in Neural Information Processing Systems*, 37:112459–  
 593 112504, 2024.

594

595 Niklas Ekvall. A lattice approach for pricing of multivariate contingent claims. *European Journal*  
 596 *of Operational Research*, 91(2):214–228, 1996.

597

598 Wendell H Fleming and Jerome L Stein. Stochastic optimal control, international finance and debt.  
 599 *Journal of Banking & Finance*, 28(5):979–996, 2004.

600

601 Alex Gorodetsky, Sertac Karaman, and Youssef Marzouk. High-dimensional stochastic optimal  
 602 control using continuous tensor decompositions. *The International Journal of Robotics Research*,  
 603 37(2-3):340–377, 2018.

594 Ludovic Goudenege, Andrea Molent, and Antonino Zanette. Machine learning for pricing american  
 595 options in high-dimensional markovian and non-markovian models. *Quantitative Finance*, 20(4):  
 596 573–591, 2020.

597

598 Jiequn Han et al. Deep learning approximation for stochastic control problems. *arXiv preprint*  
 599 *arXiv:1611.07422*, 2016.

600 Carsten Hartmann and Christof Schütte. Efficient rare event simulation by optimal nonequilibrium  
 601 forcing. *Journal of Statistical Mechanics: Theory and Experiment*, 2012(11):P11004, 2012.

602

603 Carsten Hartmann, Ralf Banisch, Marco Sarich, Tomasz Badowski, and Christof Schütte. Charac-  
 604 terization of rare events in molecular dynamics. *Entropy*, 16(1):350–376, 2013.

605 Michael B Haugh and Leonid Kogan. Pricing american options: A duality approach. *Operations*  
 606 *Research*, 52(2):258–270, 2004.

607

608 Onésimo Hernández-Lerma and Jean B Lasserre. *Discrete-time Markov control processes: basic*  
 609 *optimality criteria*, volume 30. Springer Science & Business Media, 2012.

610 Lars Holdijk, Yuanqi Du, Ferry Hooft, Priyank Jaini, Berend Ensing, and Max Welling. Stochastic  
 611 optimal control for collective variable free sampling of molecular transition paths. *Advances in*  
 612 *Neural Information Processing Systems*, 36:79540–79556, 2023.

613

614 Shashi Jain and Cornelis W Oosterlee. Pricing high-dimensional bermudan options using the  
 615 stochastic grid method. *International Journal of Computer Mathematics*, 89(9):1186–1211, 2012.

616 Jan Kallsen. Stochastic Optimal Control in Mathematical Finance. Lecture Notes (WS2015/16),  
 617 2016.

618

619 Michael Kohler, Adam Krzyżak, and Nebojsa Todorović. Pricing of high-dimensional american  
 620 options by neural networks. *Mathematical Finance*, 20(3):383–410, 2010.

621 Damien Lamberton and Bernard Lapeyre. *Introduction to stochastic calculus applied to finance*.  
 622 Chapman and Hall/CRC, 2011.

623

624 Michel Ledoux and Michel Talagrand. *Probability in Banach Spaces: isoperimetry and processes*,  
 625 volume 23. Springer Science & Business Media, 1991.

626

627 Jérémie Lelong. Dual pricing of american options by wiener chaos expansion. *SIAM Journal on*  
 628 *Financial Mathematics*, 9(2):493–519, 2018.

629

630 Pierre-Louis Lions and Henri Regnier. Calcul du prix et des sensibilités d'une option américaine par  
 631 une méthode de monte carlo, 2. *Preprint*, 2001.

632

633 Francis A Longstaff and Eduardo S Schwartz. Valuing american options by simulation: a simple  
 634 least-squares approach. *The Review of Financial Studies*, 14(1):113–147, 2001.

635

636 Pascal Massart. Some applications of concentration inequalities to statistics. In *Annales de la*  
 637 *Faculté des sciences de Toulouse: Mathématiques*, volume 9, pp. 245–303, 2000.

638

639 Giacomo Meanti, Luigi Carratino, Lorenzo Rosasco, and Alessandro Rudi. Kernel methods through  
 640 the roof: handling billions of points efficiently. *Advances in Neural Information Processing*  
 641 *Systems*, 33:14410–14422, 2020.

642

643 Sanjoy K Mitter. Filtering and stochastic control: A historical perspective. *IEEE Control Systems*  
 644 *Magazine*, 16(3):67–76, 2002.

645

646 Michael A Nielsen. *Neural networks and deep learning*, volume 25. Determination press San  
 647 Francisco, CA, USA, 2015.

648

649 Goran Peskir and Albert Shiryaev. *Optimal stopping and free-boundary problems*. Springer, 2006.

650

651 Huyêñ Pham. *Continuous-time stochastic control and optimization with financial applications*, vol-  
 652 ume 61. Springer Science & Business Media, 2009.

648 Martin L Puterman. *Markov decision processes: discrete stochastic dynamic programming*. John  
 649 Wiley & Sons, 2014.  
 650

651 Sebastian Reich. Data assimilation: the schrödinger perspective. *Acta Numerica*, 28:635–711, 2019.  
 652

653 Daniel Revuz and Marc Yor. *Continuous martingales and Brownian motion*, volume 293. Springer  
 654 Science & Business Media, 2013.  
 655

656 Lorenz Richter and Julius Berner. Improved sampling via learned diffusions. *arXiv preprint  
 657 arXiv:2307.01198*, 2023.  
 658

659 L. C. G Rogers. Monte carlo valuation of american options. *Mathematical Finance*, 12(3):271–286,  
 660 2002.  
 661

662 Alessandro Rudi, Raffaello Camoriano, and Lorenzo Rosasco. Less is more: Nyström computational  
 663 regularization. *arXiv preprint arXiv:1507.04717*, 28, 2015a.  
 664

665 Alessandro Rudi, Raffaello Camoriano, and Lorenzo Rosasco. Less is More: Nyström Computa-  
 666 tional Regularization. December 2015b.  
 667

668 Shai Shalev-Shwartz and Shai Ben-David. *Understanding machine learning: From theory to algo-  
 669 rithms*. Cambridge university press, 2014.  
 670

671 Steve Smale and Ding-Xuan Zhou. Estimating the approximation error in learning theory. *Analysis  
 672 and Applications*, 1(01):17–41, 2003.  
 673

674 Steve Smale and Ding-Xuan Zhou. Learning theory estimates via integral operators and their ap-  
 675 proximations. *Constructive approximation*, 26(2):153–172, 2007.  
 676

677 Ingo Steinwart and Andreas Christmann. *Support vector machines*. Springer Science & Business  
 678 Media, 2008a.  
 679

680 Ingo Steinwart and Andreas Christmann. *Support Vector Machines*. Springer Science & Business  
 681 Media, September 2008b. ISBN 978-0-387-77242-4. Google-Books-ID: HUnqnrpYt4IC.  
 682

683 Ingo Steinwart, Don R Hush, Clint Scovel, et al. Optimal rates for regularized least squares regres-  
 684 sion. In *COLT*, pp. 79–93, 2009.  
 685

686 Richard S Sutton, Andrew G Barto, et al. *Reinforcement learning: An introduction*, volume 1. MIT  
 687 press Cambridge, 1998.  
 688

689 Evangelos Theodorou, Freek Stulp, Jonas Buchli, and Stefan Schaal. An iterative path integral  
 690 stochastic optimal control approach for learning robotic tasks. *IFAC Proceedings Volumes*, 44(1):  
 691 11594–11601, 2011.  
 692

693 John N Tsitsiklis and Benjamin Van Roy. Optimal stopping of markov processes: Hilbert space the-  
 694 ory, approximation algorithms, and an application to pricing high-dimensional financial deriva-  
 695 tives. *IEEE Transactions on Automatic Control*, 44(10):1840–1851, 1999.  
 696

697 Francisco Vargas, Will Grathwohl, and Arnaud Doucet. Denoising diffusion samplers. *arXiv  
 698 preprint arXiv:2302.13834*, 2023.  
 699

700 Cédric Villani et al. *Optimal transport: old and new*, volume 338. Springer, 2008.  
 701

702 Christopher Williams and Matthias Seeger. Using the nyström method to speed up kernel machines.  
 703 *Advances in neural information processing systems*, 13, 2000.  
 704

705 Christopher KI Williams and Carl Edward Rasmussen. *Gaussian processes for machine learning*,  
 706 volume 2. MIT press Cambridge, MA, 2006.  
 707

708 Qinsheng Zhang and Yongxin Chen. Path integral sampler: a stochastic control approach for sam-  
 709 pling. *arXiv preprint arXiv:2111.15141*, 2021.  
 710

711 Tong Zhang. Learning bounds for kernel regression using effective data dimensionality. *Neural  
 712 Computation*, 17(9):2077–2098, 2005.  
 713

714 Wei Zhang, Han Wang, Carsten Hartmann, Marcus Weber, and Christof Schütte. Applications of the  
 715 cross-entropy method to importance sampling and optimal control of diffusions. *SIAM Journal  
 716 on Scientific Computing*, 36(6):A2654–A2672, 2014.  
 717

702 **A AUXILIARY LEMMAS**  
 703

704 In this section, we prove a number of technical results that are instrumental for establishing the  
 705 theoretical properties of our Bellman recursion in  $L^2_{\mu_t}$  spaces. In particular, we aim to verify that  
 706 the Bellman operator  $\mathcal{T}_t$  is well defined and Lipschitz continuous under mild assumptions. These  
 707 properties are essential for proving stability and convergence of our value function approximations.

708 We begin with a useful lemma on the behavior of essential suprema, which allows us to control  
 709 expressions of the form  $\text{ess sup}_{u \in U_t} \{F_t(\cdot, u) + P_t^u g\}$  arising in the Bellman operator.

710 **Lemma 1.** *Let  $\{Y_a\}_{a \in A}$  and  $\{Z_a\}_{a \in A}$  be two collections of random variables indexed by a pa-  
 711 rameter set  $A$ , such that  $\text{ess sup}_{a \in A} |Y_a| < \infty$  and  $\text{ess sup}_{a \in A} |Z_a| < \infty$  almost surely. Then the  
 712 following inequalities hold almost surely:*

$$714 \quad \left| \text{ess sup}_{a \in A} (Y_a + Z_a) \right| \leq \text{ess sup}_{a \in A} |Y_a| + \text{ess sup}_{a \in A} |Z_a|, \quad (32)$$

$$716 \quad \left| \text{ess sup}_{a \in A} Y_a - \text{ess sup}_{a \in A} Z_a \right| \leq \text{ess sup}_{a \in A} |Y_a - Z_a|. \quad (33)$$

719 *Proof.* The first bound follows from the general inequality  $|\text{ess sup}_{a \in A} Y_a| \leq \text{ess sup}_{a \in A} |Y_a|$ .  
 720 For the second inequality, we exploit the invariance under translations: the statement holds  
 721 if we replace  $Y_a$  and  $Z_a$  by  $Y_a + C$  and  $Z_a + C$ , for any random variable  $C$ . Choosing  
 722  $C = \max\{\text{ess sup}_{a \in A} (-Y_a), \text{ess sup}_{a \in A} (-Z_a)\}$ , we can assume without loss of generality  
 723 that  $Y_a, Z_a \geq 0$ . Then we obtain from Eq. 32 that  $\text{ess sup}_{a \in A} Y_a \leq \text{ess sup}_{a \in A} |Y_a - Z_a| +$   
 724  $\text{ess sup}_{a \in A} Z_a$ , and same for  $Y_a$  and  $Z_a$  exchanged, which proves Eq. 33.  $\square$

725 With this result in hand, we now analyze the properties of the Bellman operator  $\mathcal{T}_t$  as defined in  
 726 Eq. 6. The following lemma shows that, under suitable assumptions,  $\mathcal{T}_t$  maps  $L^2_{\mu_{t+1}}$  to  $L^2_{\mu_t}$  in a  
 727 controlled way and satisfies a global Lipschitz bound.

728 **Lemma 2.** *Under conditions 8 in Assumption 1, the Bellman operator  $\mathcal{T}_t$  defines a Lipschitz con-  
 729 tinuous map satisfying:*

$$731 \quad \|\mathcal{T}_t g\|_{L^2_{\mu_t}} \leq c_F + c_P^{1/2} \|g\|_{L^2_{\mu_{t+1}}}, \quad (34)$$

$$732 \quad \|\mathcal{T}_t g - \mathcal{T}_t f\|_{L^2_{\mu_t}}^2 \leq c_P \|g - f\|_{L^2_{\mu_{t+1}}}^2, \quad (35)$$

734 for all  $g, f \in L^2_{\mu_{t+1}}$  and  $t = 0, \dots, T - 1$ .

736 *Proof.* We begin by bounding the operator norm:

$$737 \quad \begin{aligned} \|\mathcal{T}_t g\|_{L^2_{\mu_t}} &= \left\| \text{ess sup}_{u \in U_t} \{F_t(\cdot, u) + P_t^u g\} \right\|_{L^2_{\mu_t}} \\ 738 &\leq \left\| \text{ess sup}_{u \in U_t} |F_t(\cdot, u)| + \text{ess sup}_{u \in U_t} |P_t^u g| \right\|_{L^2_{\mu_t}} \\ 739 &\leq \left\| \text{ess sup}_{u \in U_t} |F_t(\cdot, u)| \right\|_{L^2_{\mu_t}} + \left\| \text{ess sup}_{u \in U_t} |P_t^u g| \right\|_{L^2_{\mu_t}} \\ 740 &\leq c_F + c_P^{1/2} \|g\|_{L^2_{\mu_{t+1}}}, \end{aligned}$$

747 where we used Lemma 1 and Assumption 1. For the Lipschitz property, we compute:

$$748 \quad \begin{aligned} \|\mathcal{T}_t g - \mathcal{T}_t f\|_{L^2_{\mu_t}} &= \left\| \text{ess sup}_{u \in U_t} \{F_t(\cdot, u) + P_t^u g\} - \text{ess sup}_{u \in U_t} \{F_t(\cdot, u) + P_t^u f\} \right\|_{L^2_{\mu_t}} \\ 749 &\leq \left\| \text{ess sup}_{u \in U_t} |P_t^u(g - f)| \right\|_{L^2_{\mu_t}} \\ 750 &\leq c_P^{1/2} \|g - f\|_{L^2_{\mu_{t+1}}}, \end{aligned}$$

755 again applying Lemma 1 and that  $P_t^u$  is a linear operator.  $\square$

756 **B TECHNICAL DETAILS ON SECTION 4**  
 757

758 **B.1 TERM I**  
 759

760 In this section, we give further details about the analysis of our learning-based approximation  
 761 scheme in Section 4.

762 We start with the optimal learning rates established for regularized empirical risk minimization in  
 763 RKHS. The following theorem is taken from Steinwart et al. (2009).

764 **Theorem** (Steinwart et al. (2009, Theorem 1)). *Let  $k$  be a bounded measurable kernel on  $X$  with  
 765  $\|k\|_\infty = 1$  and separable RKHS  $\mathcal{H}$ . Let*

766 
$$A_q(\lambda) := \inf_{f \in \mathcal{H}} (\lambda \|f\|_{\mathcal{H}}^q + \mathcal{R}(f) - \mathcal{R}^*). \quad (36)$$

767 Moreover, let  $P$  be a distribution on  $X \times [-B, B]$ , where  $B > 0$  is some constant. For  $\nu = P_X$   
 768 assume that the extended sequence of eigenvalues of the integral operator satisfies

769 
$$\mu_i(L_k) \leq ai^{-\frac{1}{p}}, \quad i \geq 1, \quad (37)$$

770 where  $a \geq 16M^4$  and  $p \in (0, 1)$ . Assume further that there exist constants  $C \geq 1$  and  $s \in (0, 1]$   
 771 such that

772 
$$\|f\|_\infty \leq C \|f\|_{\mathcal{H}}^s \cdot \|f\|_{L_2(P_X)}^{1-s} \quad (38)$$

773 for all  $f \in \mathcal{H}$ . Then, for all  $q \geq 1$ , there exists a constant  $c_{p,q}$  depending only on  $p$  and  $q$  such that  
 774 for all  $\lambda \in (0, 1]$ ,  $\tau > 0$ , and  $n \geq 1$ , with probability at least  $1 - 3e^{-\tau}$

775 
$$\mathcal{R}(\hat{f}_\lambda) - \mathcal{R}^* \leq 9A_q(\lambda) + c_{p,q} \left( \frac{a^{pq} B^{2q}}{\lambda^{2p} n^q} \right)^{\frac{1}{q-2p+pq}} + \frac{120C^2 B^{2-2s}\tau}{n} \left( \frac{A_q(\lambda)}{\lambda} \right)^{\frac{2s}{q}} + \frac{3516B^2\tau}{n} \quad (39)$$

776 with  $\mathcal{R}^* := \mathcal{R}(f^*)$  the risk of the Bayes function  $f^* \in L^2(P_X)$  and  $\hat{f}_\lambda$  the data dependent estimator  
 777 from ERM algorithm.

778 Note that Eq 37 is exactly the condition mentioned under Eq. 25. We give here more details on  
 779 the connection with the *capacity assumption*. Before defining it, we define the so-called *effective  
 780 dimension* (Zhang, 2005; Caponnetto & De Vito, 2007), for  $\alpha > 0$ , as

781 
$$d_\alpha = \text{Tr}((L_k + \alpha I)^{-1} L_k) = \sum_j \frac{\sigma_j}{\sigma_j + \alpha} \quad (40)$$

782 where  $(\sigma_j)_j$  are the strictly positive eigenvalues of  $L_k$ , with eigenvalues counted with respect to  
 783 their multiplicity and ordered in a non-increasing way, and  $(u_j)$  is the corresponding family of  
 784 eigenvectors.

785 **Assumption 4** (Capacity Assumption). *There exist constants  $p \geq 1$  and  $Q > 0$  such that, for all  
 786  $\alpha \in (0, 1]$*

787 
$$d_\alpha \leq Q\alpha^{-1/p}.$$

788 This assumption, standard in statistical learning theory (see Caponnetto & De Vito, 2007; Smale  
 789 & Zhou, 2007), is often referred to as a capacity condition, as it quantifies the effective size of the  
 790 RKHS via the decay of the eigenvalues of the integral operator  $L_k$  (see Proposition 1 and 2 below).  
 791 Note that the case  $p = 1$  corresponds to no spectral assumption (i.e. the weakest possible capacity  
 792 control), which is the setting we adopt in the main text.

793 The following two results provide a tight bound on the effective dimension under the assumption  
 794 of a polynomial decay or an exponential decay of the eigenvalues  $\sigma_j$  of  $L_k$ . Since the covariance  
 795 operator  $\Sigma$  and the integral operator  $L_k$  share the same eigenvalues, we equivalently report known  
 796 proofs for  $\Sigma$  in the following.

797 **Proposition 1** (Polynomial eigenvalues decay Caponnetto & De Vito (2007, Proposition 3)). *If for  
 798 some  $\gamma \in \mathbb{R}^+$  and  $1 < p < +\infty$*

799 
$$\sigma_i \leq \gamma i^{-p}$$

800 *then*

801 
$$d_\alpha \leq \gamma \frac{p}{p-1} \alpha^{-1/p} \quad (41)$$

810 *Proof.* Since the function  $\sigma/(\sigma + \alpha)$  is increasing in  $\sigma$  and using the spectral theorem  $\Sigma = UDU^*$   
 811 combined with the fact that  $\text{Tr}(UDU^*) = \text{Tr}(U(U^*D)) = \text{Tr}D$

$$813 \quad d_\alpha = \text{Tr}(\Sigma(\Sigma + \alpha I)^{-1}) = \sum_{i=1}^{\infty} \frac{\sigma_i}{\sigma_i + \alpha} \leq \sum_{i=1}^{\infty} \frac{\gamma}{\gamma + i^p \alpha} \quad (42)$$

816 The function  $\gamma/(\gamma + x^p \alpha)$  is positive and decreasing, so

$$817 \quad d_\alpha \leq \int_0^{\infty} \frac{\gamma}{\gamma + x^p \alpha} dx \\ 818 \quad = \alpha^{-1/p} \int_0^{\infty} \frac{\gamma}{\gamma + \tau^p} d\tau \\ 819 \quad \leq \gamma \frac{p}{p-1} \alpha^{-1/p} \quad (43)$$

824 since  $\int_0^{\infty} (\gamma + \tau^p)^{-1} d\tau \leq p/(p-1)$ .  $\square$

826 A similar result, leading to even faster rates, can be obtained assuming an exponential decay.

827 **Proposition 2** (Exponential eigenvalues decay Della Vecchia et al. (2024, Proposition 3)). *If for*  
 828 *some  $\gamma, p \in \mathbb{R}^+$   $\sigma_i \leq \gamma e^{-pi}$  then*

$$829 \quad d_\alpha \leq \frac{\log(1 + \gamma/\alpha)}{p} \quad (44)$$

832 *Proof.*

$$834 \quad d_\alpha = \sum_{i=1}^{\infty} \frac{\sigma_i}{\sigma_i + \alpha} = \sum_{i=1}^{\infty} \frac{1}{1 + \alpha/\sigma_i} \leq \sum_{i=1}^{\infty} \frac{1}{1 + \alpha' e^{pi}} \leq \int_0^{+\infty} \frac{1}{1 + \alpha' e^{px}} dx \quad (45)$$

837 where  $\alpha' = \alpha/\gamma$ . Using the change of variables  $t = e^{px}$  we get

$$839 \quad (45) = \frac{1}{p} \int_1^{+\infty} \frac{1}{1 + \alpha' t} \frac{1}{t} dt = \frac{1}{p} \int_1^{+\infty} \left[ \frac{1}{t} - \frac{\alpha'}{1 + \alpha' t} \right] dt = \frac{1}{p} \left[ \log t - \log(1 + \alpha' t) \right]_1^{+\infty} \\ 840 \quad = \frac{1}{p} \left[ \log \left( \frac{t}{1 + \alpha' t} \right) \right]_1^{+\infty} = \frac{1}{p} \left[ \log(1/\alpha') + \log(1 + \alpha') \right] \quad (46)$$

843 So we finally obtain

$$845 \quad d_\alpha \leq \frac{1}{p} \left[ \log(\gamma/\alpha) + \log(1 + \alpha/\gamma) \right] = \frac{\log(1 + \gamma/\alpha)}{p} \quad (47)$$

848  $\square$

849 Specializing this result to ridge regression, and under an additional approximation condition on the  
 850 learning target, we obtain a more explicit convergence rate in terms of the sample size.

852 **Corollary** (Steinwart et al. (2009, Corollary 6)). *Assume  $s = p = 1$ ,  $q = 2$ , and suppose the*  
 853 *2-approximation error function satisfies*

$$854 \quad A_2(\lambda) \leq c\lambda^\beta, \quad \lambda > 0 \quad (48)$$

856 for some constants  $c > 0$  and  $\beta > 0$ . Define a sequence of regularization parameters  $\lambda := n^{-\frac{1}{\beta+1}}$ .  
 857 Then there exists a constant  $K \geq 1$  depending only on  $a$ ,  $B$ , and  $c$ , such that for all  $\tau \geq 1$  and  
 858  $n \geq 1$ ,

$$859 \quad \mathcal{R}(\hat{f}_\lambda) - \mathcal{R}(f^*) \leq K\tau n^{-\frac{\beta}{\beta+1}} \quad (49)$$

861 with probability at least  $1 - 3e^{-\tau n^{\frac{\beta}{\beta+1}}}$ .

863 This is the result reported in Theorem 1, given that source condition in Assumption 3 implies condition in Eq.48 as shown in Smale & Zhou (2003).

864 B.2 TERM II  
865866 We start by defining the empirical Rademacher complexity:  
867

868 
$$\widehat{\mathcal{R}}(\mathcal{F}_t^x) := \mathbb{E}_\sigma \sup_{f \in \mathcal{F}_t^x} \left| \frac{1}{M_t} \sum_{i=1}^{M_t} \sigma_i f(z_i) \right|, \quad (50)$$
  
869

870 with  $\sigma_1, \dots, \sigma_{M_t}$  independent Rademacher variables, i.e.  $\mathbb{P}(\sigma_i = 1) = \mathbb{P}(\sigma_i = -1) = 1/2$ .  
871872 To control the empirical approximation error uniformly over a function class, we rely on the following  
873 concentration inequality due to Boucheron et al. (2005).  
874875 **Lemma** (Boucheron et al. (2005, Theorem 3.2)). *Let  $X_1, \dots, X_n$  be i.i.d. random variables in a  
876 set  $\mathcal{X}$  and let  $\mathcal{F}$  be a class of functions  $\mathcal{X} \rightarrow [-1, 1]$ . Then, with probability at least  $1 - \delta$ ,*  
877

878 
$$\sup_{f \in \mathcal{F}} \left| \mathbb{E} f(X) - \frac{1}{n} \sum_{i=1}^n f(X_i) \right| \leq 2\widehat{\mathcal{R}}(\mathcal{F}(X_1^n)) + \sqrt{\frac{2 \log \frac{1}{\delta}}{n}}, \quad (51)$$
  
879

880 with  
881

882 
$$\widehat{\mathcal{R}}(A) = \mathbb{E} \sup_{a \in A} \frac{1}{n} \left| \sum_{i=1}^n \sigma_i a_i \right|, \quad (52)$$
  
883

884 where  $A \subset \mathbb{R}^n$  and  $\mathcal{F}(x_1^n)$  is the class of vectors  $(f(x_1), \dots, f(x_n))$  for  $f \in \mathcal{F}$ .  
885886 We also have:  
887

888 
$$\sup_{f \in \mathcal{F}} \left| \mathbb{E} f(X) - \frac{1}{n} \sum_{i=1}^n f(X_i) \right| \leq 2\widehat{\mathcal{R}}(\mathcal{F}(X_1^n)) + \sqrt{\frac{2 \log \frac{2}{\delta}}{n}}. \quad (53)$$
  
889

890 There are several well-studied cases in which the Rademacher complexity can be upper bounded.  
891 We highlight two such cases that are particularly relevant for the financial applications of interest  
892 here.  
893894 • Using Massart's Lemma (Massart, 2000): if  $\mathcal{F}_t^x$  is finite, i.e.,  $\mathcal{F}_t^x = \{f_1, \dots, f_K\}$ , then  
895

896 
$$\mathbb{E}\widehat{\mathcal{R}}(\mathcal{F}_t^x) \lesssim \sqrt{\frac{\log K}{M_t}}. \quad (54)$$
  
897

898 This result is particularly relevant for our application to American options, as the control  
899 set  $\mathcal{U}_t = \{0, 1\}$  is finite at each time step  $t$ .  
900901 • Using Talagrand's Contraction Lemma (Ledoux & Talagrand, 1991): if  $\mathcal{F}_t^x$  is not finite,  
902  $\widehat{W}_{t+1}^{\lambda_{t+1}}$  is  $L_W$ -Lipschitz, and we define  $\Pi_t^x := \{z \mapsto \pi_t(x, u, z) : u \in \mathcal{U}_t\}$ , then the com-  
903 position class  $\mathcal{F}_t^x = \widehat{W}_{t+1}^{\lambda_{t+1}} \circ \Pi_t^x$  satisfies  
904

905 
$$\widehat{\mathcal{R}}(\mathcal{F}_t^x) \leq L_W \cdot \widehat{\mathcal{R}}(\Pi_t^x). \quad (55)$$
  
906

907 Assuming that  $\pi_t(x, u, z)$  is  $L_\pi$ -Lipschitz in  $u$  and applying standard covering number  
908 arguments we obtain  
909

910 
$$\mathbb{E}\widehat{\mathcal{R}}(\mathcal{F}_t^x) \lesssim \frac{L_W \cdot L_\pi}{\sqrt{M_t}}. \quad (56)$$
  
911

912 This can be useful in the continuous control case, e.g.,  $\mathcal{U}_t \subset [0, 1]$ , as the class  $\Pi_t^x$  is no  
913 longer finite.  
914915 We report the two above mentioned results.  
916917 **Lemma** (Massart's Lemma (Massart, 2000), (Shalev-Shwartz & Ben-David, 2014, Lemma 26.8)).  
918 Let  $\mathcal{F} = \{f_1, \dots, f_K\}$  be a finite class of functions satisfying  $\|f\|_\infty \leq b$  for all  $f \in \mathcal{F}$ . Then,  
919

920 
$$\widehat{\mathcal{R}}(\mathcal{F}) \leq b \sqrt{\frac{2 \log K}{n}}. \quad (57)$$
  
921

918 **Lemma** (Contraction Inequality (Bartlett & Mendelson, 2002, Thm. 12), (Ledoux & Talagrand, 919 1991, Cor. 3.17)). Let  $\mathcal{F} \subset \mathbb{R}^{\mathcal{Z}}$  be a class of real-valued functions, and let  $\phi_1, \dots, \phi_n : \mathbb{R} \rightarrow \mathbb{R}$  be 920  $L$ -Lipschitz functions. Let  $S = \{z_1, \dots, z_n\} \subset \mathcal{Z}$  be a fixed sample. Then

$$\mathbb{E}_{\sigma} \left[ \sup_{f \in \mathcal{F}} \frac{1}{n} \sum_{i=1}^n \sigma_i \phi_i(f(z_i)) \right] \leq L \cdot \mathbb{E}_{\sigma} \left[ \sup_{f \in \mathcal{F}} \frac{1}{n} \sum_{i=1}^n \sigma_i f(z_i) \right], \quad (58)$$

925 where  $\sigma_1, \dots, \sigma_n$  are independent Rademacher random variables.

### 927 B.3 FINAL BOUND

929 Given the above upper bounds on the three terms in Eq. 23, and choosing  $\lambda \sim n^{-\frac{1}{\beta_t+1}}$ , we have 930 with high probability

$$\mathcal{E}_t \lesssim \left( \frac{1}{n_t} \right)^{\frac{\beta_t}{\beta_t+1}} + \frac{1}{M_t} + c_P \mathcal{E}_{t+1}. \quad (59)$$

935 Selecting  $M_t \sim n_t^{\frac{\beta_t}{\beta_t+1}}$  gives the result in Theorem 1.

## 937 C NUMERICAL SIMULATIONS

940 Firstly, we briefly describe the benchmark methods used for comparison in Tables 1 and 2, following 941 Goudenege et al. (2020).

942 **GPR-Tree.** This method combines Gaussian Process Regression (GPR) with a tree-based exercise 943 strategy. At each time step, the continuation value is estimated using GPR, and a decision tree 944 determines whether to exercise or continue. The method is designed to reduce variance and improve 945 interpretability, particularly in low-dimensional settings. We report the results from (Goudenege 946 et al., 2020, Tables 1–3) using  $P = 1000$  training points, which offers the highest reported accuracy 947 despite increased computational cost compared to  $P = 250$  or  $P = 500$ .

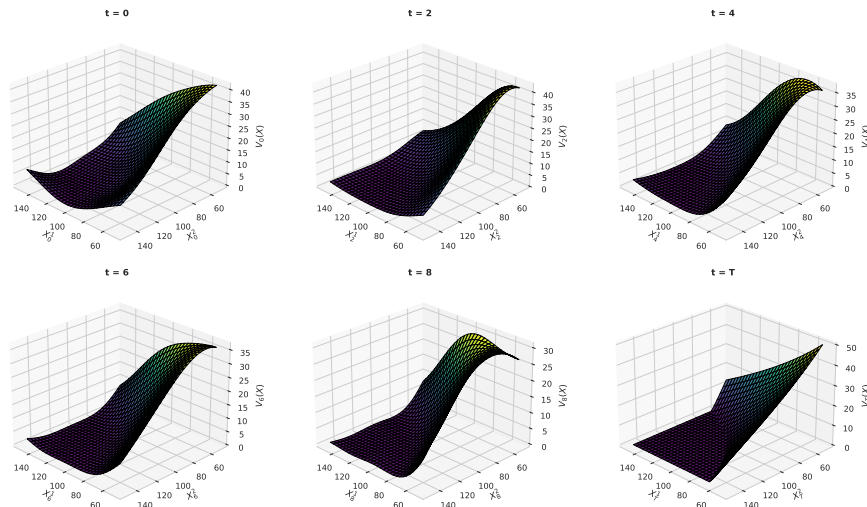
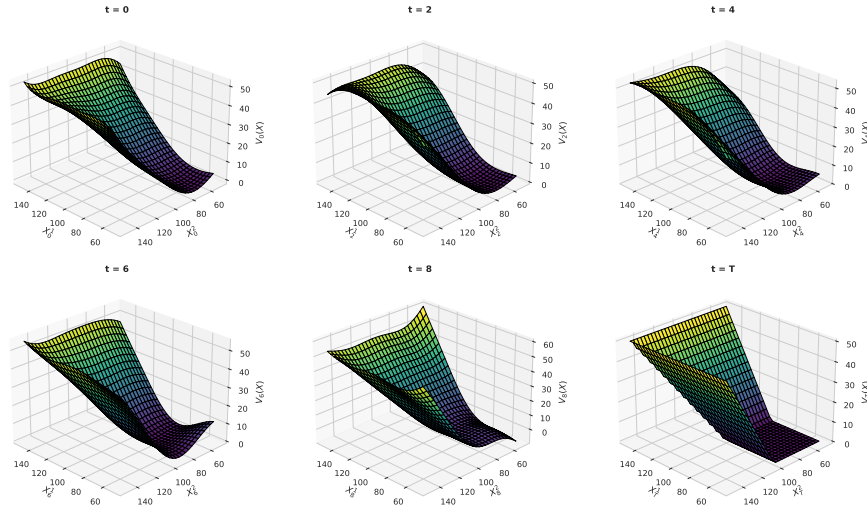
949 **GPR-EI.** GPR with Expected Improvement (EI) follows a sequential design strategy inspired by 950 Bayesian optimization. It actively selects the most informative sample points by maximizing ex- 951 pected improvement in the value function, enabling a more data-efficient approximation of the 952 continuation value. As with GPR-Tree, we report the results with  $P = 1000$  training points.

954 **GPR-MC.** This variant uses GPR to estimate the continuation value within a standard Monte Carlo 955 regression framework. It replaces linear regression with nonparametric GPR to improve accuracy, 956 especially in high-dimensional problems.

958 **Ekval.** This baseline method is based on the lattice-based regression approach proposed in Ekval 959 (1996), which approximates the value function using basis functions and optimal stopping. It serves 960 as a classical benchmark for evaluating newer machine learning-based methods.

962 **Benchmark.** A closed-form analytical solution is available only for the Geometric Basket Put 963 option.

965 **Our method.** We kept a basic implementation, exploiting classic libraries. We report the av- 966 erage performance of our method over 10 repetitions, along with corresponding confidence inter- 967 vals. The regularization parameter is simply set to  $\lambda = 10^{-6}$ , and the RBF kernel lengthscale 968 is selected from the grid  $\{40, 80\}$ . Sample sizes increase with dimensionality; for instance: for 969  $d = 2$ , we use  $n = 200$ ,  $M = 50$ ; for  $d = 20$ , we use  $n = 800$ ,  $M = 100$ . All experiments 970 were run on Google Colab using an NVIDIA T4 GPU (16 GB) with a single Intel Xeon CPU 971 and approximately 12 GB of RAM. The FALKON algorithm (Meanti et al., 2020) is taken from 972 <https://github.com/FalkonML/falkon>.

Figure 1: Value function estimates for the Geometric Basket Put option ( $d = 2$ ), see Table 1.Figure 2: Value function estimates for the Max-Call option ( $d = 2$ ), see Table 2.

## D SUFFICIENT CONDITIONS FOR WELL-POSEDNESS

We discuss here the minimal condition needed for our formulation to be well posed in relation to Assumption 1. Given a function  $f \in L^2_{\mu_{t+1}}$ , we study under which condition  $P_t^u f$  belongs to  $L^2_{\mu_t}$ , with

$$P_t^u f(x) = \int_{\mathcal{X}_{t+1}} f(x') P_t^u(x, dx'). \quad (60)$$

Using Jensen's inequality:

$$\|P_t^u f\|_{L^2_{\mu_t}}^2 = \int_{\mathcal{X}_t} \left( \int_{\mathcal{X}_{t+1}} f(x') P_t^u(x, dx') \right)^2 \mu_t(dx) \leq \int_{\mathcal{X}_{t+1}} f(x')^2 \underbrace{\int_{\mathcal{X}_t} P_t^u(x, dx') \mu_t(dx)}_{=: q_t^u(dx')} . \quad (61)$$

1026 If the pushforward measure  $q_t^u$  is absolutely continuous with respect to  $\mu_{t+1}$  and admits a bounded  
 1027 Radon–Nikodym derivative, i.e.,  
 1028

$$1029 \quad \left\| \frac{dq_t^u}{d\mu_{t+1}} \right\|_{L_{\mu_{t+1}}^\infty} \leq c_P < \infty, \quad (62)$$

1031 then we obtain:

$$1033 \quad \|P_t^u f\|_{L_{\mu_t}^2} \leq c_P^{1/2} \|f\|_{L_{\mu_{t+1}}^2}, \quad (63)$$

1034 which is exactly the requirement in Assumption 1.

1035 Although condition 63 may appear strong, it can often be verified in applications. Indeed, observe  
 1036 that

$$1038 \quad \|f\|_{L_{\mu_{t+1}}^2}^2 = \int_{\mathcal{X}_t} \mathbb{E} [f(\pi_t(x, \bar{u}_t(x), Z_{t+1}))^2] \mu_t(dx). \quad (64)$$

1039 Therefore, a sufficient structural condition for 63 to hold is the pointwise inequality:

$$1041 \quad \sup_{u \in \mathcal{U}_t} \mathbb{E} [f(\pi_t(x, u, Z_{t+1}))]^2 \leq c_{P,t}^2 \mathbb{E} [f(\pi_t(x, \bar{u}_t(x), Z_{t+1}))^2], \quad \text{for } \mu_t\text{-a.e. } x \in \mathcal{X}_t. \quad (65)$$

1043 This provides a more verifiable condition for establishing Assumption 1, especially in simulation-  
 1044 based settings where the behavior distribution is known or controlled.

1045  
 1046  
 1047  
 1048  
 1049  
 1050  
 1051  
 1052  
 1053  
 1054  
 1055  
 1056  
 1057  
 1058  
 1059  
 1060  
 1061  
 1062  
 1063  
 1064  
 1065  
 1066  
 1067  
 1068  
 1069  
 1070  
 1071  
 1072  
 1073  
 1074  
 1075  
 1076  
 1077  
 1078  
 1079